Central European Journal of Energetic Materials
ISSN 1733-7178; e-ISSN 2353-1843

Cent. Eur. J. Energ. Mater. 2024, *21*(2): 171-187; DOI 10.22211/cejem/190439
Article is available in PDF-format, in colour, at:
https://ipo.lukasiewicz.gov.pl/wydawnictwa/cejem-woluminy/vol-21-nr-2/

Research paper

Verification of Impact Energy Delivered by a Drop Weight

Martin Künzel*), **Jindrich Kucera**, **Jakub Smid**, **Jan Horkel**
OZM Research, Bliznovice 32, Hrochuv Tynec, Czech Republic
* *E-mail:* kunzel.martin@gmail.com

Abstract: Impact sensitivity of energetic materials is an important parameter for their safe handling and storage. The drop height or equivalent potential energy that is required to reach a certain probability of initiation in repeated tests is determined using a drop-weight instrument. In this work, photonic Doppler velocimetry was used to measure the drop weight velocity profile during its fall and rebound. Numerical simulations were performed to correctly understand the velocity records and to find out the differences from the ideal behavior. The efficiency of the conversion from the potential to kinetic energy was revealed for various drop weight masses and drop heights. The measured velocities at the moment of impact followed the free-fall predictions to within 1%. The energy conversion efficiency decreased from 0.997 to 0.992 with the drop weight decrease from 10 to 0.5 kg. The relative energies of the rebound drop-weights decreased with decreasing mass from >0.75 at 2-10 kg down to <0.4 at 0.5 kg. The PDV instrumentation was found useful for validating the drop-weight velocity. The resting times and rebound velocity profiles of the drop-weights agreed with the numerical simulation results that assumed elastic behavior of the instrument.

Keywords: impact sensitivity, drop-weight, BAM Fall Hammer, photonic Doppler velocimetry

1 Introduction

Impact sensitivity of explosives is determined by the statistical evaluation of a number of attempts to initiate a sample with a weight falling from various heights using a drop-weight tester (also BAM Fall Hammer or BAM Impact Tester) [1]. Some testing procedures are designed to find a certain height to reach a specified probability of explosion [2], while others allow finding a dependence of the explosion probability on the input energy [3-5]. The drop height or equivalent potential energy corresponding to 50% probability of initiation (E_{50}) is usually used as a measure of impact sensitivity [6]. Despite the widespread use of the impact testers, the exact mechanism of impact initiation is still not fully understood. Significant advances in its understanding have been made thanks to the use of instrumented drop-weight testers [7] and photographic studies of impact events using glass anvils [8]. It has been experimentally confirmed that the amount of energy actually utilized in a sample initiation is only a fraction of the energy supplied by the falling weight. Optical velocimetry instrumentation was recommended for future studies of the impact initiation phenomena [9].

Assuming the energy conservation law, the original potential energy of the weight is transformed into the kinetic energy which is then delivered to the sample at the moment of impact. The energy losses due to air drag and friction of the rails are neglected in practice but may in fact differ in different instruments and even within individual drop-weights in the same instrument. That contributes to the overall spread of results that may be quite high even in the case of well-known samples and well-described testing procedure [10]. In a recent paper [11], the energy conversion factors defined as the ratios of the measured and theoretical kinetic energy of about 0.95 were found that gradually decreased down to 0.85 at the lowest drop height of 10 cm. In another paper [12], much higher efficiencies of over 0.97 were found. Both papers used pairs of simple optical sensors to measure average free fall velocity within a certain interval.

In this work, we followed up on our previous attempts [13] and utilized photonic Doppler velocimetry (PDV) [14] to record full velocity-time profiles of the drop-weight impact event. This allowed us to measure the impact velocities, efficiencies and to reveal the rebound behavior in an uncompromised way. The velocity profiles have been obtained for various drop heights and drop-weight masses.

2 Experimental

2.1 The impact tester

The BAM Fall Hammer BFH 12 produced by OZM Research was used in the tests (Figure 1) with drop-weight masses of 0.5, 1, 2, 5 and 10 kg. The drop-weights (except the 0.5 kg, which had a different design) have brass grooves sliding on stainless steel guide rails. No oil was applied on the rails. The 0.5 kg and 1 kg weights have a two-mass body while the others are made of rectangular blocks of metal (Figure 2). The instrument uses an electromagnetic release mechanism for the weight that allows simple operation and provides a trigger pulse for the velocity measurement.

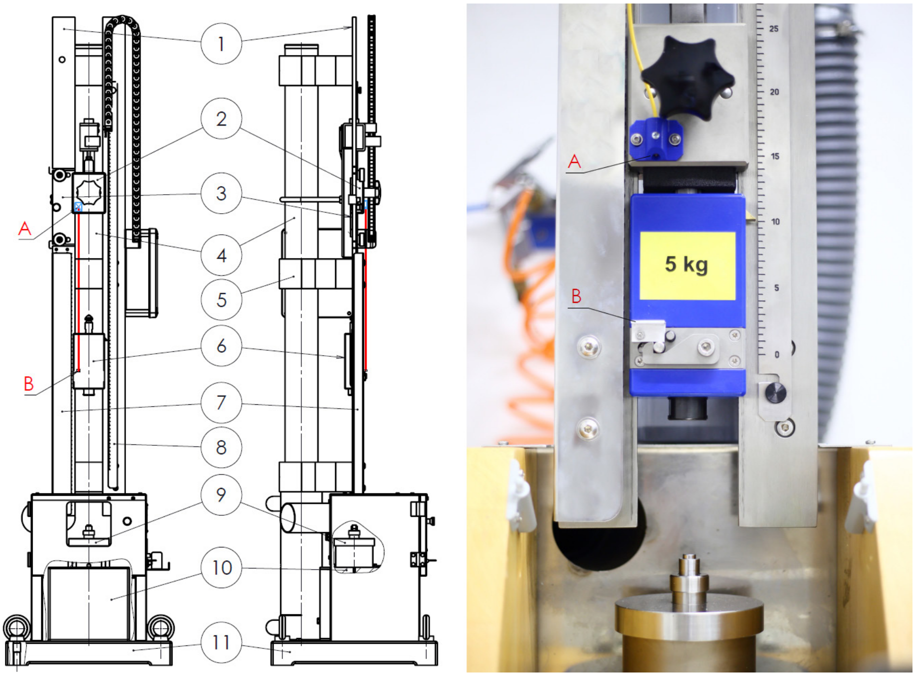

Figure 1. A scheme and a detailed photo of the measurement setup. The impact tester consists of: 1 – guide rails, 2 – a release device, 3 – a drop-weight exchange window, 4 – a column, 5 – three cross-pieces, 6 – a drop-weight, 7 – a tooth rack, 8 – a ruler, 9 – a main anvil and 10, 11 – a pedestal (The PDV probe (A) is aimed at the retroreflector holder (B), which is fixed to the drop-weight.)

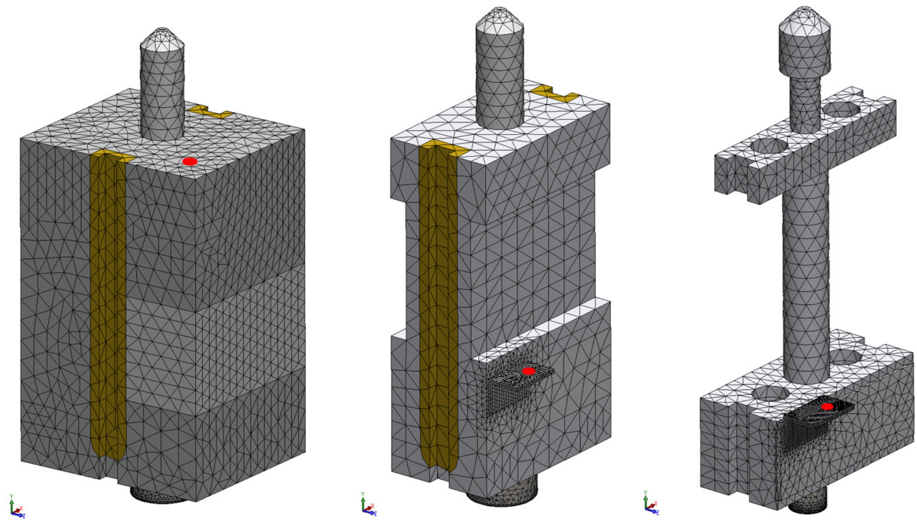

Figure 2. Finite element models of 10, 2 and 0.5 kg drop-weights divided into mesh elements (The nodes used in the simulations are marked with red dots (see the electronic version).)

2.2 Velocity measurement

The drop weight velocity was measured using VeloreX PDV photonic Doppler velocimeter produced by OZM Research. The 1550 nm laser light was directed onto the weight by means of a parallel beam probe with the laser power of 16-75 mW. In order not to interfere with the drop weight construction, the probe was fixed on the side of the release device using a custom made holder. The probe was pointed downwards in a way that its optical axis ran along the front surface of the drop weight. An aluminum holder with retroreflective self-adhesive tape was attached to the drop weight in the laser beam path. The measurement was triggered externally by a voltage signal which controlled the release device. The voltage signals from the PDV were recorded using TDS2038 or DPO70404C digital oscilloscopes (Tektronix).

The oscilloscope records were converted to the velocity-time profiles using Short-Time Fourier Transform (STFT) using WinSpeed software. Two different sets of STFT parameters were used for evaluating of the complete falling path and the moment of impact (Table 1). The impact velocity was determined as the last time point of the velocity profile before the impact corresponding to the last 82 μs or 0.1-0.25 mm of the fall path. The real drop heights were determined through numerical integration of the velocity-time profiles.

Table 1. STFT evaluation parameters

Event	Window length (Samples)	Overlap [%]	Zero padding
Free fall	4092	50	4x
Impact	128	50	16x

2.3 Data evaluation

The measured impact velocities were used to calculate the drop-hammer efficiency and the relative rebound energy. The efficiency (q) was defined as the ratio of the measured to the theoretical impact energy (squared velocities) according to Equation 1.

$$q = v_I^2 / v_T^2 \tag{1}$$

where v_I and v_T are the experimental and theoretical impact velocities, respectively. The theoretical velocity was calculated assuming free-fall, *i.e.* no air resistance and no friction using Equation 2.

$$v_T = \sqrt{2gh} \tag{2}$$

where g is gravitational acceleration of 9.8105 m/s^2 (latitude 49.96° N) and h is the nominal drop height. A correction for the true drop height was performed by using integral value of the velocity profile instead of the nominal value. Another correction was attempted for air drag using Equations 3 and 4.

$$v_C = v_L \sqrt{1 - exp\left[\frac{-2gh}{v_L^2}\right]} \tag{3}$$

$$v_L = \sqrt{\frac{2mg}{C\rho A}} \tag{4}$$

where v_C is the corrected impact velocity, v_L is the limiting velocity of the weight with the projected frontal area A, mass m and aerodynamic drag coefficient C. The medium density of ρ = 1.2 kg/m^3 was used for air at 20 °C and 40% relative humidity. The drag coefficient was pessimistically estimated to be 1.05 which corresponds to a cube freely falling in ambient air with its bottom surface parallel to the ground. The relative rebound energy (k) was calculated using Equation 5.

$$k = v_I^2 / v_R^2 \tag{5}$$

where the initial rebound velocity (v_R) was read out from the regression line of the deceleration phase at the moment of impact.

2.4 Numerical simulations

For comparison with experimental results of drop weight impacts, numerical simulations using finite element method (FEM) were carried out for the 0.5 kg, 2 kg and 10 kg drop-weights. Impact analysis was performed using SolidWorks Simulation Professional software [15] which includes a special module, Drop Test Analysis, specifically designed for modelling the impact force of short-duration mechanical structure events.

The analysis described herein was preprocessed as a fully linear-elastic, meaning there was no energy dissipation due to material plastic deformation, damping and friction. The model was simplified by removing geometry features insignificant for analysis (external fillets, rounds, logos, etc.). Velocity profiles were obtained at the simulation nodes identical with the points on the holders illuminated by the PDV probe (Figure 2).

Key parameters for the analysis are the densities ρ and Young's modules E of the drop-weight materials (Table 2). The impact device was modeled as a fictitious flexible spring with the stiffness equivalent to that of two cylinders.

Each model in the analysis was excited by a simulated free fall impact. The fall height was 0.5 m with initial velocity equal to zero and no rotations/vibrations were considered until initial impact occurs. Simulation time starting from the impact was 500 μs. The time duration depends on velocity of elastic shock wave generated by the impact and the corresponding roundtrip distance within the drop-weight body. Value of the shock wave velocity is established based on geometry and material properties which stem from Equation 6.

$$v_{Elastic\,wave} = \sqrt{\frac{E}{\rho}} \tag{6}$$

For the processing procedure, the explicit solver with direct integration and automatic time step incrementation was used. Solid quadratic tetrahedral mesh with eight nodes was utilized, each node has three degrees of freedom.

Table 2. Parameters of the drop weight materials obtained from the reference [16]

Item	Drop-weight heads (all)	Drop-weight body (5 and 10 kg)	Drop-weight body (0.5, 1 and 2 kg)	Impact cylinders
Material	1.2842	1.0038	EN AW-7075 T6	100Cr6
E [MPa]	$2 \cdot 10^5$	$2.1 \cdot 10^5$	$0.717 \cdot 10^5$	$2.05 \cdot 10^5$
ρ [kg/m^3]	7610	7850	2810	7810

3 Results and Discussion

3.1 Measurements

A total number of 73 measurements with various drop-weight masses and fall heights were performed and evaluated. The PDV instrumentation allowed for detailed analysis of the drop weight movement in a great detail. An example velocity spectrogram obtained from the STFT evaluation contains is shown in Figure 3. It shows gradual acceleration of the drop-weight until the point of impact where the velocity trace suddenly drops to zero at the time of impact and then jumps back up to show the rebound velocity. In the rebound phase, the slope if the velocity profile is negative, indicating that the drop-weight decelerates. In this deceleration phase, the catch mechanism repeatedly strikes the rack next to the rail, inducing vibrations in the drop-weight body. The deceleration continues until zero velocity, at which point the drop-weight reverses the direction and freely falls down to the nearest stopping teeth of the rack. The discussion is divided into three sections which follow the operation procedure of the impact tester.

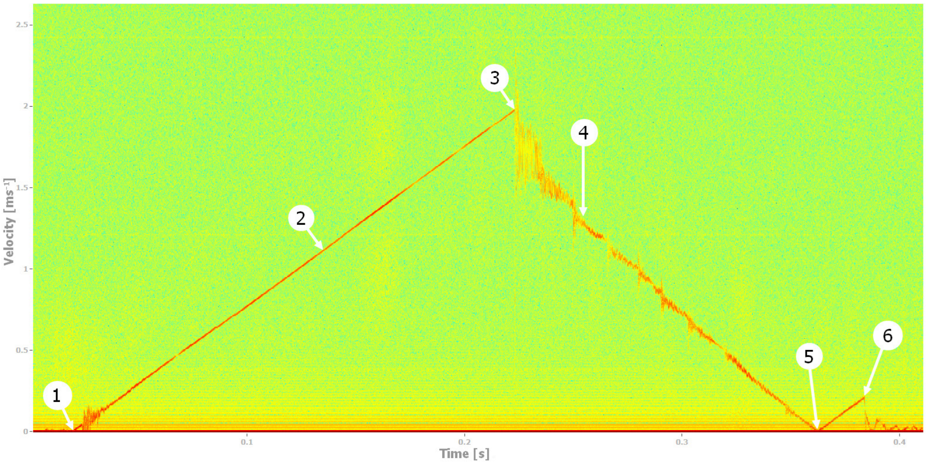

Figure 3. A typical complete drop-weight velocity spectrogram obtained using the PDV (The drop-weight release (1) is followed by a free fall (acceleration) phase (2) that ends at the moment of impact (3). The rebound drop-weight deceleration (4) shows periodic oscillations due to the rebound catch mechanism action. After the drop-weight reaches its peak height (5), it falls down to the nearest teeth and comes to a stop (6).)

3.2 The release and fall

After a delay required for opening the release mechanism, the drop weight begins to fall due to the force of gravity. The initial part of the velocity profile always contains some oscillations caused by vibrations of the release device (Figure 4). In the two-mass drop weights, the oscillations are stronger and persist until the impact. The time period of these velocity oscillations during the fall is about 1.25 and 0.67 ms for the 0.5 and 1 kg weight, respectively. That compares well with the simulated values of 1.17 ms for the 1st natural frequency of the 1 kg drop-weight and 0.66 ms for the 3rd natural frequency of the 0.5 kg drop-weight. In the other weights, the oscillations are only visible up to the fall distance of about 1.5 mm and it is unclear whether they are caused by the drop weight itself, the release device or a combination. All the natural frequencies of these drop-weights are too high to be captured by the current setup.

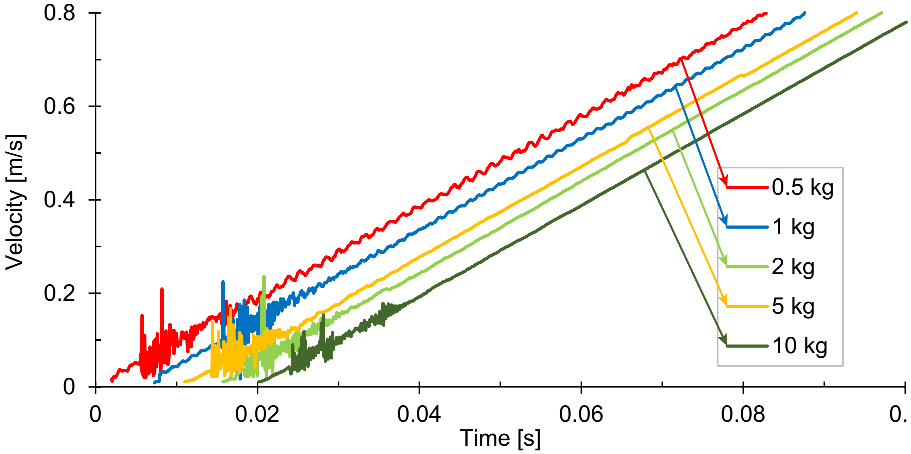

Figure 4. Detailed view of the initial part of the velocity profiles showing persistent oscillations in 0.5 and 1 kg drop-weights (The time span corresponds to the first ~3 mm of the movement. The lines are artificially shifted in time for clarity.)

According to the Newtonian mechanics, the impact velocity depends on the fall height and the force of gravity. It can be negatively influenced by air drag and friction force with the rails. The true fall heights were determined by integration of the velocity profiles and used to calculate theoretical maximum velocity values corresponding to the individual experiments shown in the Figure 5 (triangles). These velocities are about 0.1% below the nominal maximum velocity as the true fall heights were all lower than the nominal value set on the instrument. The difference is attributed to backlash of the release device and manufacturing tolerances. The additional air drag correction according to Equation 3 slightly shifts the values of the 0.5 and 1 kg weights while the difference in the case of heavier weights is negligible. Therefore, the remaining difference in the measured velocity compared to the calculated value of 0.2-0.4% must be mostly attributed to the friction force.

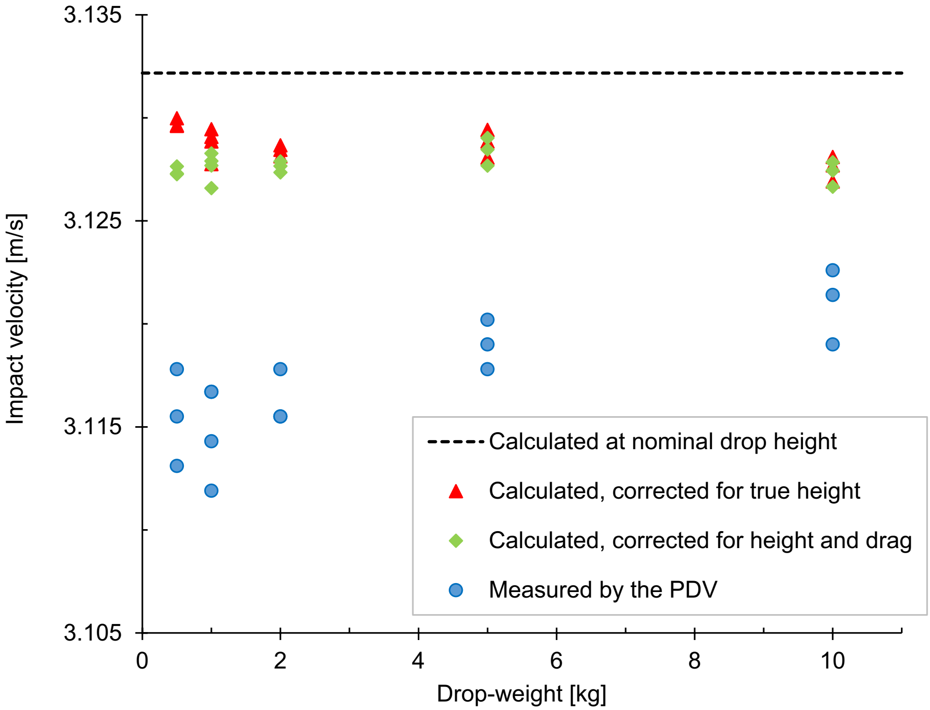

Figure 5. Measured impact velocities compared to the theoretical maximum value (Equation 2) and corrected experimental values (Equation 3). (The figure demonstrates that the difference in measured velocity cannot be attributed to the true height or the air resistance.)

It can be seen from the Figures 6 and 7 that all the efficiencies were higher than 0.99, *i.e.* comparable to those in [12] and significantly higher than those in [11]. It seems that there is a systematic error in the calculation of q in [11] due to an incorrect correction of the fall height – the average free fall velocity was measured within the interval of 25 and 5 mm before the impact but the calculated velocity corresponded to the point 5 mm before impact instead of 15 mm.

In the present work, no significant dependence of the efficiency on the drop height was found. The effect of mass is visible but the deviation from ideal behavior is within 1% for all the drop-weights. It seems that the absence of brass grooves in the 0.5 kg drop-weight has no effect on the efficiency, as it fits in the trend.

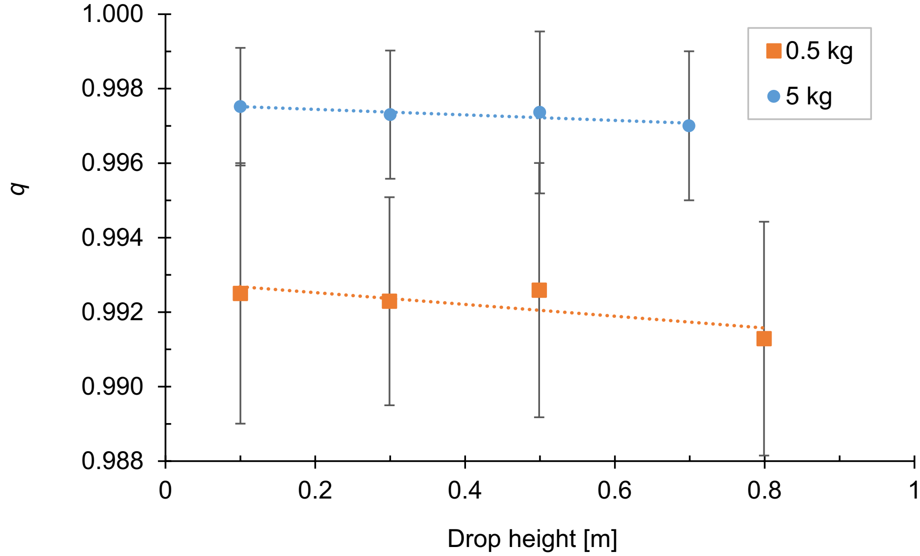

Figure 6. Efficiencies, q, of 0.5 and 5 kg drop-weights falling from different heights (There is a clear difference of these two masses and a much smaller effect of varying height. The uncertainty is shown as twice the standard deviation of five tests.)

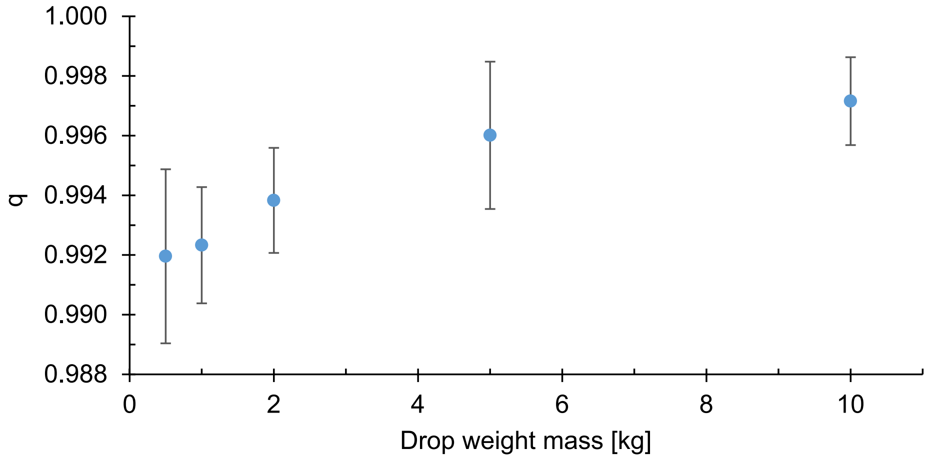

Figure 7. Efficiencies of drop-weights of various masses falling from a height of 0.5 m (The efficiency gradually decreases with the decreasing mass. The uncertainty is shown as twice the standard deviation of at least six tests.)

3.3 The moment of impact

The moment of impact manifests in the velocity profiles as a momentary drop from the maximum to zero velocity (Figure 8). The falling edge of the profile has a finite duration due to the elastic behavior of the drop weight, impact device, and pedestal. The FEM simulations revealed that the impact device gets compressed by as much as 0.3 mm when loaded. However, the cylinders used in testing were checked with a micrometer after the tests, and there were no changes in dimensions, indicating that there was no measurable plastic deformation even after repeated impacts. The FEM simulations further explained the observed intense velocity oscillations after the rebound. They were primarily caused by the presence of the retroreflector holder. However, in the case of the 0.5 kg drop-weight, the combined effect of the holder and the two-mass construction amplified the oscillations even more. The resting times of the drop weights were in good agreement with the simulated values and showed an approximately linear dependence on mass (Figure 9), which also confirms elastic behavior.

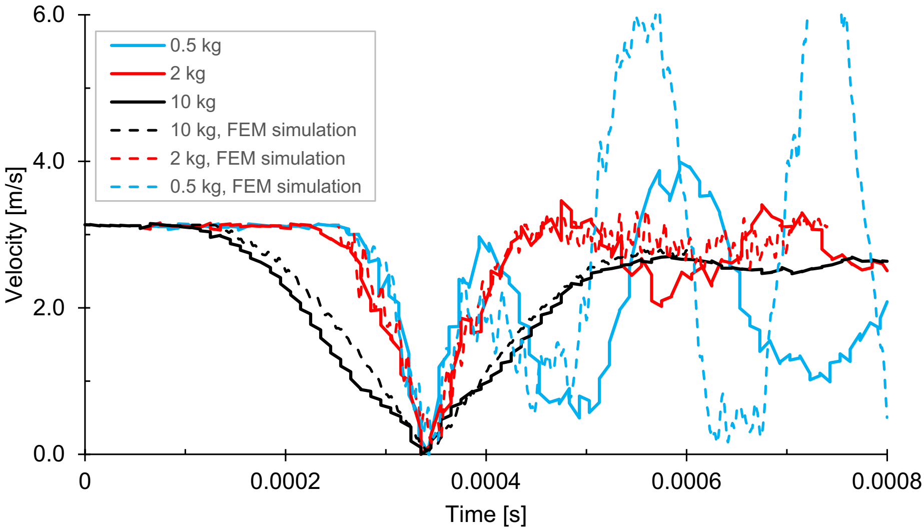

Figure 8. Detailed view of example velocity profiles of the 0.5, 2 and 10 kg drop-weights at the moment of impact compared to their simulations (moving average of 5 points)

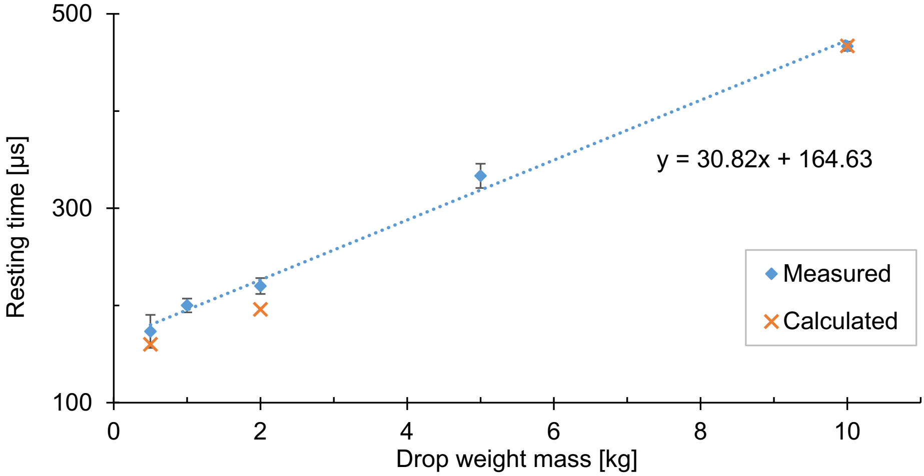

Figure 9. Resting times of the drop-weights compared to the simulated values (The uncertainty is shown as twice the standard deviation of 3 tests.)

3.4 Rebound

The latter part of the velocity profile shows the drop-weight deceleration while moving upwards. Due to the stopping effect of the tooth rack, the deceleration proceeds faster than the acceleration, during which the slope is equal to the *g* constant. The smoothness of the profiles is evidently very much affected by the drop-weight construction. The rectangular drop-weights (2, 5 and 10 kg) exhibit much slower deceleration in the rebound phase than the two-mass drop-weights (0.5 and 1 kg) as can be seen from their linear regression slopes (Figure 10). In the latter, the energy is dissipated in their vibrations, which manifest as extreme velocity oscillations. Some vibrations are also visible in the 2 and 5 kg rectangular drop-weight profiles, but according to our FEM simulations (Figure 8), these were only caused by the retroreflective foil holder that was not rigid enough. The best rebound behavior (the least negative slope of 13.8 m/s^2) is obtained with the 5 kg drop-weight which is in agreement with the authors' subjective observation that this hammer is usually stopped at the highest positions of all. For further testing, the use of an external holder is not recommended – the PDV probe should be mounted in the base or at the release device to target the drop-weight bodies themselves. In the case of the 10 kg drop-weight, the rebound profile is almost clean.

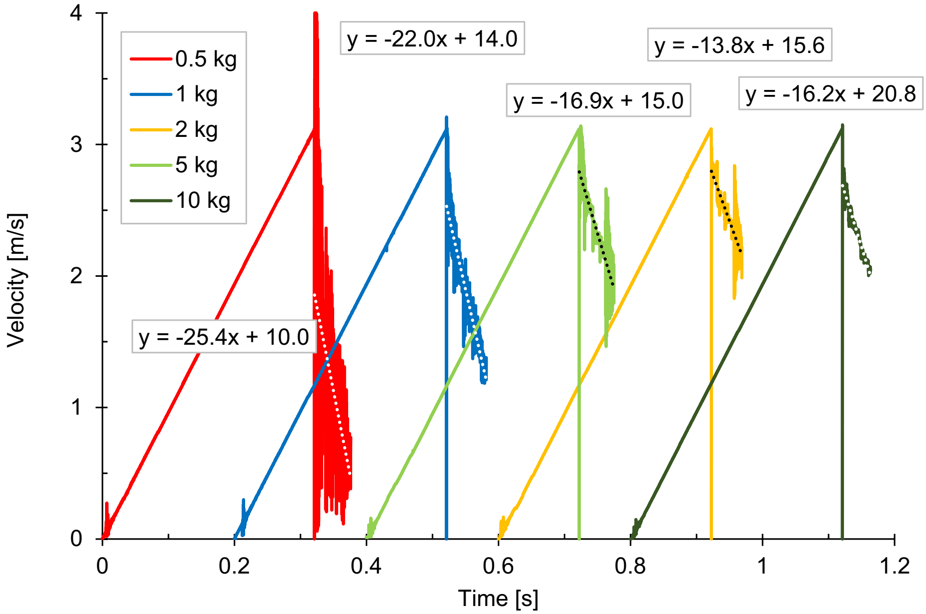

Figure 10. Examples of drop-weight velocity profiles from the tests at 0.5 m drop height (The slopes represent decelerations (in m/s^2). The deceleration phases are not complete due to limited record length. The data sets are artificially shifted in time for clarity.)

The value of *k* depends on build and installation quality of a drop-weight instrument and it typically ranges from 0.6 to 0.75 for the drop-weight masses of 1-10 kg [11]. The results for two different data sets with a constant drop height of 0.5 m and a constant energy of 4 J are shown in the Figure 11. At the constant energy loading, which was relatively low (corresponds to 10 kg drop-weight falling from 4 cm), the rebound increased with increasing mass. On the other hand, at a medium drop height of 0.5 m, the highest rebound was reached with the 2 and 5 kg drop-weights, while the 10 kg drop-weight possibly loses a minor portion of energy due to the plastic deformation of the anvil or pedestal.

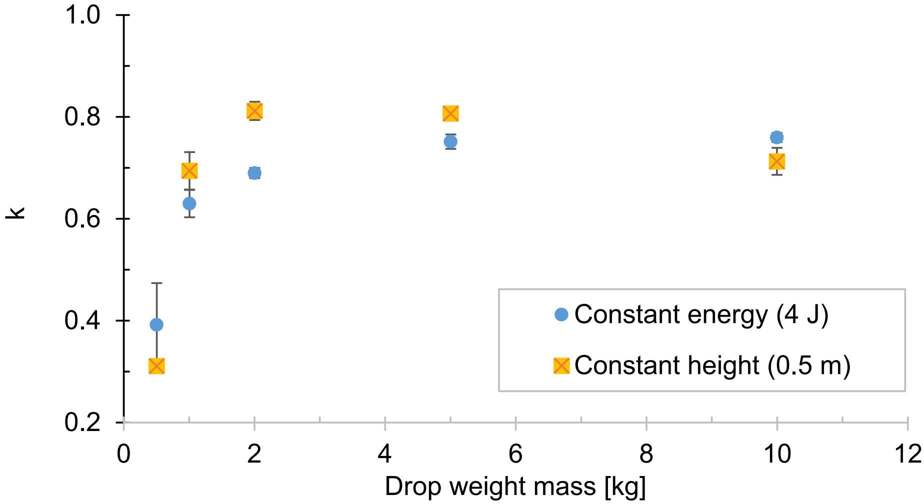

Figure 11. Relative energies of the rebound drop-weights at constant energy and constant drop height (At low energies, the rebound improves with mass. At a medium drop height of 0.5 m, the highest rebound is reached with the 2 and 5 kg drop-weights. The uncertainty is shown as twice the standard deviation of 3 tests.)

4 Conclusions

- The photonic Doppler velocimetry was used to record drop-weight velocity profiles with high time resolution. It allowed us to observe the behavior of the impact tester with unprecedented accuracy. In our tests, the efficiencies of all the falling drop weights were better than 0.99 and they only slightly decreased with decreasing drop-weight mass. No significant dependence of the efficiency on the fall height was found.
- The relative rebound energies of the two-mass drop-weights were much lower compared to the other rectangular drop-weights due to energy losses from vibrations.
- To obtain clean velocity profiles in the rebound phase, aiming the laser directly on the drop-weight body is recommended.
- Further research into the use of PDV to quantify the true energy spent in sample initiation is ongoing.

References

[1] Sućeska, M. *Test Method for Explosives* Springer-Verlag, New York, USA, **1995**; ISBN 978-0387945552.

[2] Dixon, J.W.; Mood, A.M. A Method for Obtaining and Analyzing Sensitivity Data. *J. Am. Stat. Assoc.* **1948**, *43*(241): 109-126; https://doi.org/10.2307/2280071.

[3] Šelešovský, J.; Pachman, J. Probit Analysis – A Promising Tool for Evaluation of Explosive's Sensitivity. *Cent. Eur. J. Energ. Mater.* **2010**, *7*(3): 269-277.

[4] Neyer, B.T. A D-Optimality-Based Sensitivity Test. *Technometrics* **1994**, *36*(1): 61-70; https://doi.org/10.1080/00401706.1994.10485401.

[5] Šelešovský, J.; Pelikán, V.; Schuster, J.; Janovsky, B.; Matyás, R. FEST – New Procedure for Evaluation of Sensitivity Experiments. *Propellants Explos. Pyrotech.* **2020**, *45*(11): 1813-1818; https://doi.org/10.1002/prep.202000120.

[6] Zukas, J.A.; Walters, W.P. *Explosive Effects and Applications.* Springer-Verlag, New York, **1998**; ISBN 978-0-387-98201-4.

[7] Coffey, C.S.; De Vost, V.F. Impact Testing of Explosives and Propellants. *Propellants Explos. Pyrotech.* **1995**, *20*(3): 105-115; https://doi.org/10.1002/prep.19950200302.

[8] Walley, S.M.; Field, J.E.; Biers, R.A.; Proud, W.G.; Williamson, D.M.; Jardine, A.P. The Use of Glass Anvils in Drop-Weight Studies of Energetic Materials. *Propellants Explos. Pyrotech.* **2015**. *40*(3): 351-365; https://doi.org/10.1002/prep.201500043.

[9] Rae, P.J.; Dickson, P.M. Some Observations About the Drop-weight Explosive Sensitivity Test. *J. Dyn. Behav. Mater.* **2021**, *7*: 414-424; https://doi.org/10.1007/s40870-020-00276-2.

[10] Marrs, F.W.; Manner, V.W.; Burch, A.C.; Yeager, J.D.; Brown, G.W.; Kay, L.M.; Buckley, R.T.; Anderson-Cook, C.M.; Cawkwell, M.J. Sources of Variation in Drop-weight Impact Sensitivity Testing of the Explosive Pentaerythritol Tetranitrate. *Ind. Eng. Chem. Res.* **2021**, *60*(13): 5024-5033; https://doi.org/10.1021/acs.iecr.0c06294.

[11] von Oertzen, A.; Lehmann, T. Considerations on Energy Deposition with the BAM-Fallhammer. *Cent. Eur. J. Energ. Mater.* **2016**, *13*(2): 273-288.

[12] Monogarov, K.A.; Meerov, D.B.; Fomenkov, I.V.; Pivkina, A.N. Energy Transferred to Energetic Materials During Impact Test at Reaction Threshold: Look Back to Go Forward. *FirePhysChem* **2023**, *3*(3): 255-262; https://doi.org/10.1016/j.fpc.2022.11.003.

[13] Künzel, M.; Nesvadba, P. On the Applications of Photonic Doppler Velocimetry. *Proc. 14th Int. Symp. on Explosive Production of New Materials: Science, Technology, Business and Innovations (EPNM 2018),* Saint Petersburg, Russia, **2018**.

[14] Strand, T.; Goosman, D.R.; Martinez, C.; Whitworth, T.L.; Kuhlow, W.W. Compact System for High-speed Velocimetry Using Heterodyne Techniques. *Rev. Sci. Instrum.* **2006**. *77*: paper 083108; https://doi.org/10.1063/1.2336749.

[15] *Solid Works Simulation Professional*. Dassault Systèmes Solid Works Corporation, USA, **2018**.

[16] Fiala, J.; Bebr, A.; Matoška, Z. *Engineering Tables 1 – Materials for Engineering Production.* (in Czech) SNTL – Státní nakladatelství technické literatury, Prague, Czech Republic, **1990**; ISBN 80-03-00457-8.

Received: December 23, 2023
Revised: June 25, 2024
First published online: June 28, 2024